U.P.B. Sci. Bull., Series B, Vol. 82, Iss. 2, 2020 ISSN 1454-2331

# INFLUENCE OF CONTROLLED SMELTING CONDITIONS ON THE INCLUSIONAL STATE OF SOME MARAGING STEELS

Raluca Elena GINGHINĂ[1], Tudor Viorel ȚIGĂNESCU[2], George Ovidiu IORGA[1], Ramona Monica STOICA[3], Titi PARASCHIV[3]

*Increased demand of materials with higher tensile strength determined a firm development of high strength steels, with higher hardness acquired through precipitation. Understanding the relation mechanical properties-microstructure of hardened steels remains a key topic in metallurgy and makes the object of this paper. A specific set of heat treatments leads to a successful combination tensile strength-high temperature resistance. These treatments are supposed to generate well defined microstructures able to inhibit the spread of cracks. Therefore, the second objective of the paper was to establish optimal microstructure and the appropriate heat treatment in order to manufacture materials with high strength at high temperatures.*

**Keywords**: Maraging steel, hardness materials, microscopic analysis

## 1. Introduction

The term maraging originates from the combination of two terms: martensite and aging. Precipitation-hardening steels have been developed since the 1960s. Three classes of steels have appeared and developed with uses from the most sophisticated aerospace equipment, to non-magnetic balls for pinball machines [1].

Researchers have established a niche because of their unique ability to develop high strengths through relatively simple heat treatments, without losing ductility and corrosion resistance compared to other steels with similar strength levels [2, 3]. This is possible by using one or both mechanisms: martensite formation and hardening by precipitation. Over the years, 3 basic classes of precipitation-hardening steels evolved: austenitic, martensitic and semi-austenitic. The final reinforcement mechanism in all 3 classes is precipitation hardening.

Thus, maraging steels are martensitic alloys with improved precipitation hardening with 18, 20 or 25 % nickel, a very low carbon ($C < 0.03$ %) and

---

[1] Sci. Res. 3th grade, Scientific Research Center for CBRN Defense and Ecology, Bucharest, e-mail: ginghinaraluca@gmail.com

[2] Prof., Military Equipment and Technologies Research Agency, Clinceni, e-mail: tiganescu.viorel.t@gmail.com

[1] Sci. Res. 3th grade, Scientific Research Center for CBRN Defense and Ecology, Bucharest, e-mail: iorga_ovidiu@yahoo.com

[3] Lect., Military Technical Academy, Bucharest, e-mail: ramona.stoica@mta.ro

[3] Prof., Military Technical Academy, Bucharest, e-mail: titi.paraschiv@siemens.com

hardening elements such as molybdenum, cobalt, aluminum and titanium contents. Fast-growing development of these steels is due to an entire set of very important properties such as: increased hardness, notable ductility and toughness, simple heat treatments, good welding properties, cryogenic resistance, ease to process [2 - 4].

## 2. Experimental part

### *2.1. Choosing the system of experimental materials*

The main purpose of the paper is to expand the area of usage of maraging steels in high temperature applications, beginning with a classic 300 maraging steel (tensile strength of 300 ksi) with the following average constituents in percentages: C < 0.02 %, Ni – 18 %, Co – 9 %, Mo - 4.8 %, Ti - 0,6 %, Al – 0.1 % [5].

To broaden the application field of maraging steels containing Ni, Co, Mo, Ti, Al, the concentration of Ti, Si, Al elements will be increased, the alloy with Nb and Zr will be introduced, and a temperature in the austenitic domain (over 750°C) will be used, in order to favour the formation of agglomerations of alloying elements which should strengthen the material and increase the high temperature resistance.

Experimental methodology will be focused on the following aspects [6 - 10]: - increasing the temperature of martensitic - austenitic transformation from about 500 °C to 700 – 750 °C by decreasing the concentration of Ni;

- increasing the percentage of hardening alloying elements, such as Ti, Al, Si;
- adding new hardening alloying elements: Zr and Nb.

Chemical composition of experimental batches will be in balance to avoid high concentrations of $\delta$ ferrite. The experiments were mainly focused on studying the effect of increased temperature of martensite - austenite transformation and additional alloying with Al, Zr, Nb, Si, Ti on physical and mechanical characteristics (up to 550 $^{o}$C) [10 - 13]. Chemical compositions that are aimed to be obtained are presented in Table 1:

*Table 1*

**Chemical composition aimed during experiments**

| **Chemical element** | **300 maraging standard steel** | **Transformed maraging steel** | **Maraging steel alloyed with Al-Si-Ti** | **Maraging steel alloyed with Si-Zr-Nb** |
|---|---:|---:|---:|---:|
| Nickel | 18.50 % | 12.50 % | 12.50 % | 12.50 % |
| Cobalt | 9.00 % | 9.00 % | 10.50 % | 10.50 % |
| Molybdenum | 4.80 % | 4.80 % | 4.80 % | 4.80 % |
| Titan | 0.60 % | 0.60 % | 1.50 % | 0.60 % |
| Aluminium | 0.10 % | 0.10 % | 2.50 % | 0.10 % |
| Silicon | max. 0.10 % | max. 0.10 % | 0.80 % | 1.20 % |
| Manganese | max. 0.10 % | max. 0.10 % | max. 0.10 % | max. 0.10 % |
| Carbon | max. 0.03 % | max. 0.03 % | max. 0.03 % | max. 0.03 % |

| | | | | |
|---|---|---|---|---|
| Sulphur | max. 0.01 % | max. 0.01 % | max. 0.01 % | max. 0.01 % |
| Phosphorus | max. 0.01 % | max. 0.01 % | max. 0.01 % | max. 0.01 % |
| Zirconium | - | - | - | 1.00 % |
| Niobium | - | - | - | 2.50 % |

*Table 2*

**Chemical composition of batches used in experiments**

| **Constituent [%]** | **Al** | **Ti** | **C** | **Mn** | **Ni** | **Si** | **Co** | **Mo** | **Nb** | **Zr** |
|---|---|---|---|---|---|---|---|---|---|---|
| S1Ti | 0.254 | 0.0030 | 0.015 | 1.310 | 11.43 | 1.460 | 10.17 | 5.710 | 0.0130 | <0.0006 |
| S1T2 | 3.530 | 0.0027 | 0.028 | 0.742 | 11.05 | 0.589 | 10.03 | 5.500 | 0.0124 | <0.0006 |
| S1T3 | 2.650 | 0.8000 | 0.023 | 0.657 | 10.33 | 3.060 | 12.26 | 5.090 | 0.0194 | 0.0017 |
| S2T1 | 0.250 | 0.4620 | 0.008 | 1.150 | 13.04 | 1.090 | 10.95 | 5.439 | 0.3420 | 0.0530 |
| S2T2 | 0.178 | 0.2970 | 0.005 | 1.090 | 12.39 | 1.760 | 10.87 | 5.350 | 0.7960 | 0.1630 |
| S2T3 | 0.105 | 0.0220 | 0.004 | 1.000 | 12.03 | 3.160 | 10.57 | 5.446 | 2.9700 | >0.2500 |

***Note**: Ø 60 mm casts with modifiers.*

Table 2 presents the batches chemical compositions. The chemical composition as a percentage of the tested steels is shown in Table 3.

*Table 3*

**Chemical analysis of the studied steels**

| **No.** | **Chemical element** | **Marking $M_{01}$** | **Marking Z-$S_1T_1$** | **Marking Z-$S_1T_2$** | **Marking Z-$S_1T_3$** | **Marking Z-$S_2T_1$** |
|---|---|---|---|---|---|---|
| 1 | Nickel | 17,820 | 11,5600 | 11,680 | 10,530 | 13,460 |
| 2 | Cobalt | 8,930 | 10,6200 | 10,300 | 12,500 | 11,350 |
| 3 | Molybdenum | 4,480 | 5,6200 | 5,570 | 4,970 | 5,349 |
| 4 | Titan | 0,690 | 0,0045 | 0,045 | 0,798 | 0,460 |
| 5 | Aluminium | 0,060 | 0,2680 | 3,620 | 2,780 | 0,253 |
| 6 | Silicon | 0,090 | 1,4800 | 0,560 | 3,050 | 1,040 |
| 7 | Manganese | 0,080 | 0,5330 | 0,395 | 0,295 | 0,605 |
| 8 | Carbon | 0,028 | 0,0220 | 0,028 | 0,023 | 0,006 |
| 9 | Sulphur | 0,009 | 0,0100 | 0,008 | 0,007 | 0,008 |
| 10 | Phosphorus | 0,015 | 0,0160 | 0,013 | 0,012 | 0,016 |
| 11 | Zirconium | - | 0,0050 | 0,020 | 0,050 | 0,160 |
| 12 | Niobium | - | 0,0120 | 0,012 | 0,194 | 0,350 |

**Note:** Experimental batches emptied by re-casting in arc and vacuum at Ø 100 mm

*Table 4*

**Chemical analysis of the maraging steels used to determine the high temperature characteristics**

| Chemical element | Maraging steel standard | Maraging steel transformed | Maraging steel alloyed Al-Si-Ti | Maraging steel alloyed Si-Zr-Nb |
|---|---|---|---|---|
| Nickel | 17,820 | 12,700 | 12,820 | 12,780 |
| Cobalt | 8,930 | 8,720 | 10,250 | 10,320 |
| Molybdenum | 4,480 | 4,620 | 4,740 | 4,680 |
| Titan | 0,690 | 0,480 | 1,420 | 0,540 |
| Aluminium | 0,060 | 0,080 | 2,360 | 0,070 |
| Silicon | 0,090 | 0,043 | 0,060 | 1,160 |
| Manganese | 0,080 | 0,050 | 0,070 | 0,066 |
| Carbon | 0,028 | 0,024 | 0,022 | 0,029 |
| Sulphur | 0,009 | 0,006 | 0,008 | 0,007 |
| Phosphorus | 0,015 | 0,005 | 0,007 | 0,009 |
| Zirconium | - | - | - | 0,870 |
| Niobium | - | - | - | 2,340 |

**Note:** Loads drained by re-casting in spring and vacuum Ø 100 mm

### *2.2. Study of purification process applied to maraging hardness modified steel, consisted in kettle treatment*

The purpose of the experimental tests consisted in determining the possibility of successfully replacing vacuum treatment by kettle treatment that involves applying a mix of calcium, Mischmetal (57 % Ce, 26 % La, 10 % Nd, 5 % Pr, 2 % other rare-earth elements) and magnesium. In order to analyse this possibility, charges of modified maraging steel within an air induction furnace have been prepared. Two of the charges have been tampered using the classical method with Al and another two in a furnace with ferrotitanium (0.05 %) and subsequently in a kettle with a mix of Ca, Mischmetal and Mg. Following the tampering of the liquid, batches were casted in Ø 60 mm iron moulds. Several electrodes have been made of iron moulds that have been casted using the Al classical method and of those that were treated with a mix of Ca, Mischmetal, Mg and Ti, finally melted by the vacuum method. The matrix of experiments is presented in Table 5.

*Table 5*

**Blending charges of modified maraging steel (12 % Ni)**

| Sample labelling | Tampering with Al | Treatment | |
|---|---|---|---|
| | | In kettle with Mischmetal + Mg+ Ti + Ca | In vacuum – RAV |
| **SA 1** | X | - | X |
| **SA 2** | - | X | X |
| **SA 3** | X | - | - |
| **SA 4** | - | X | - |

| | | | |
|---|---|---|---|
| **SA 5** | X | X | |

- Sample SA5 was tampered only with calcium.

**Note:** After melting in vacuum, the iron mould is Ø 100 mm in diameter

## 3. Results and analysis

Samples for gas analysis and EDAX analysis were taken from the cast ingots. The samples were taken from the most unfavourable area in terms of purity and microstructure.The samples were studied using a QUANTA INSPECT scanning electron microscope provided with field emission gas and energy dispersive X-ray spectrometer.

Further on are presented aspects regarding the microstructure of several samples.

### *3.1. The sample tampered with aluminium, prepared in air induction furnace – SA3*

The sample microstructure is highlighted due to images of scanning electron microscopy, images of secondary electrons (SE) from Fig. 1, $\alpha$ Fe - Ni solid solution grains and inclusions within grains. The sample highlights the presence of inclusions such as aluminium oxide and manganese sulphide (MnS).

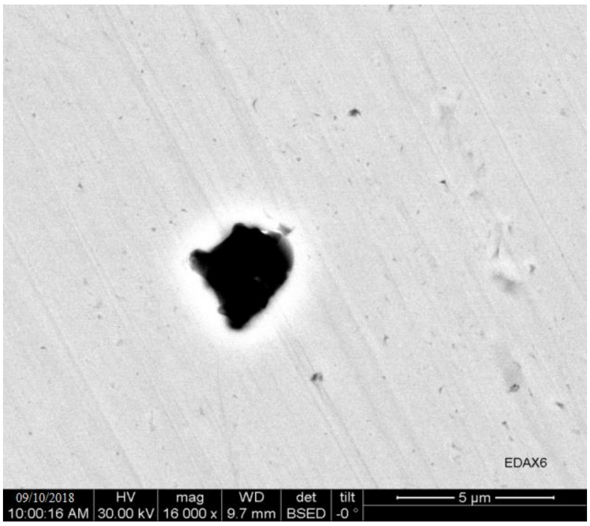

Fig. 1. Microstructural view – sample SA3 aluminium oxide and manganese sulphide (magnification - 16000x)

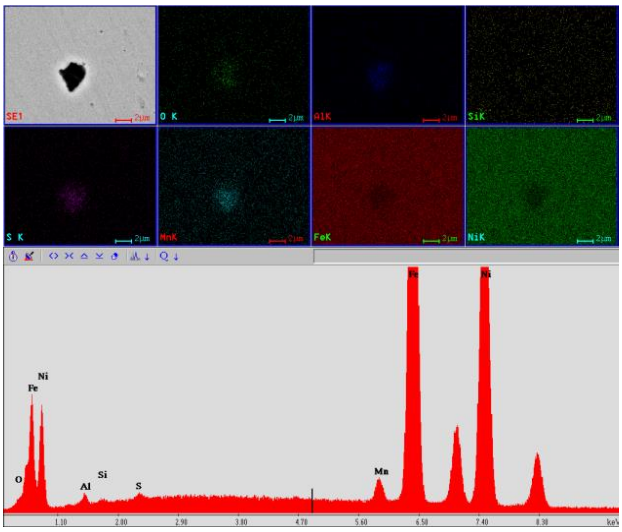

Fig. 2. Image of secondary electrons and distribution in surface of relative intensity of radiation X characteristic to MnKα, SKα, FeKα, CKα, O2Kα, AlKα, SiKα si NiKα on the micro-area from Fig. 1.

The energy dispersive X-ray spectrum of Fig. 2 and 4 shows that the sample contains the following elements: Fe and Ni (majority) but also Mn, Al, Si and S.

### 3.2. Sample treated „in kettle" with Ti, Mischmetal, Mg, Ca, prepared in air induction furnace – SA4

The sample microstructure is highlighted due to images of scanning electron microscopy, images of backscattered electrons from Fig. 5, *α* Fe - Ni solid solution grains and titanium nitride inclusions.

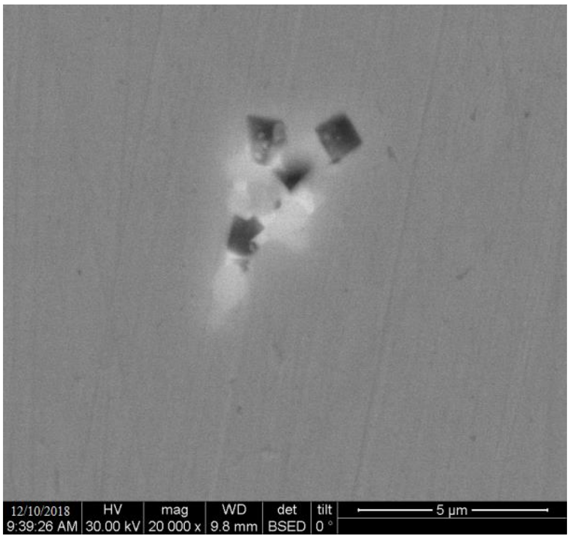

Fig. 5. Titanium nitride (magnification 20000 x)

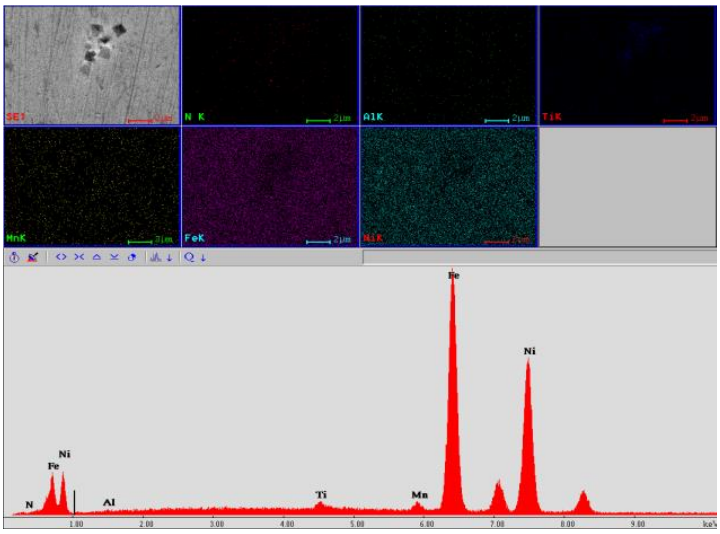

Fig. 6. Image of backscattered electrons and distribution in surface of relative intensity of radiation X characteristic to NKα, AlKα, SKα, TiKα, MnKα , FeKα,  NiKα on the micro-area from Fig. 3.

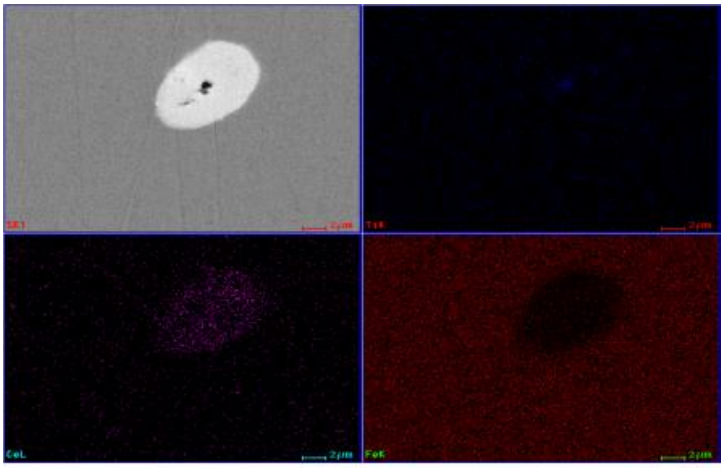

Fig. 7. Cerium and lanthanum segregation (x10000)

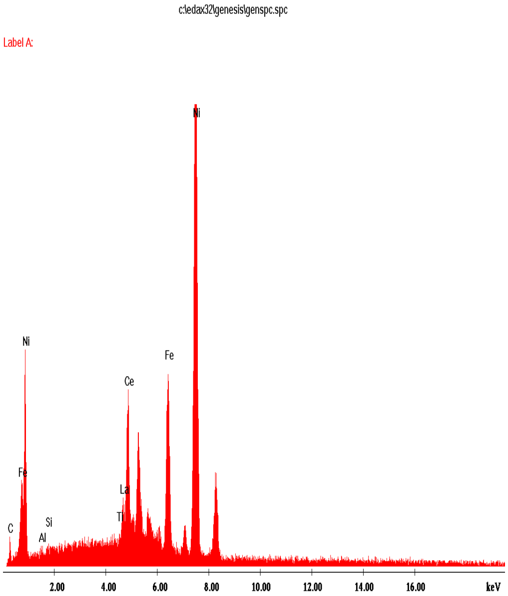

Fig. 8. Energy-dispersive X-ray spectrum associated with the microzone in Fig. 7

### *3.3. Sample tampered with aluminium, prepared in air induction furnace and follow-up melted in vacuum (RAV) – SA1*

The sample microstructure is highlighted due to images of scanning electron microscopy and images of backscattered electrons from Fig. 9, which highlights the existence of oxides in *α* solid solution. Particles that appear in dark tones are inclusions existent in α solid solution.

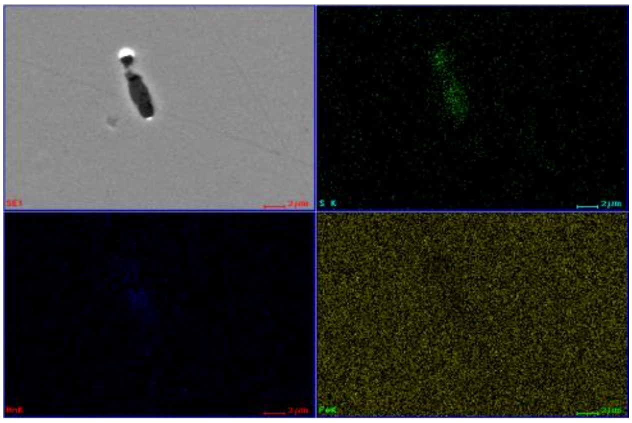

Fig. 9. Image of secondary electrons and associated surface distribution images of the relative intensity of characteristic X-radiation SKα, MnKα, FeKα, NiKα. The inclusion of manganese sulphide type is observed.

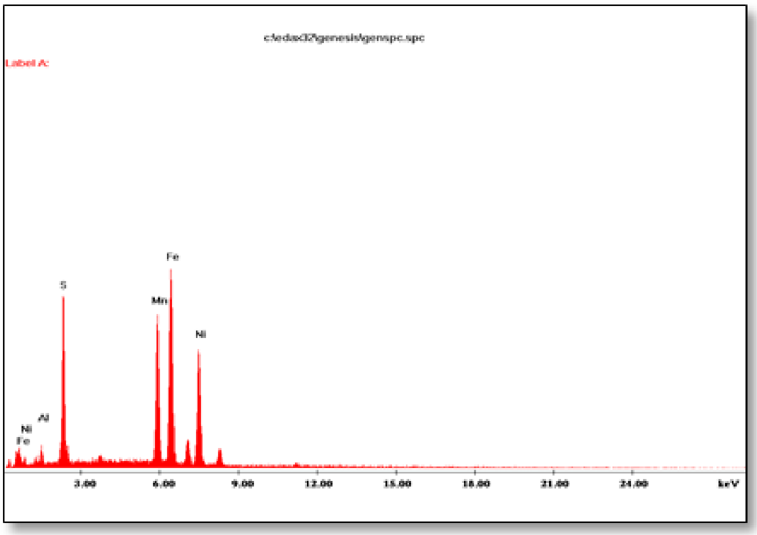

Fig. 10. Energy-dispersive X-ray (EDX) spectroscopy associated to micro-area from Fig. 9

The energy-dispersive X-ray spectroscopy (EDX) from Fig. 10 shows that the sample contains both primary elements such as Fe and Ni and an area with high concentration of S and Mn, which can point out the existence of manganese sulphide [6].

### 3.4. Sample treated „in kettle” with Cu, Ti, Mischmetal, Mg, Ca, prepared in air induction furnace and vacuum remelted (RAV) – SA2

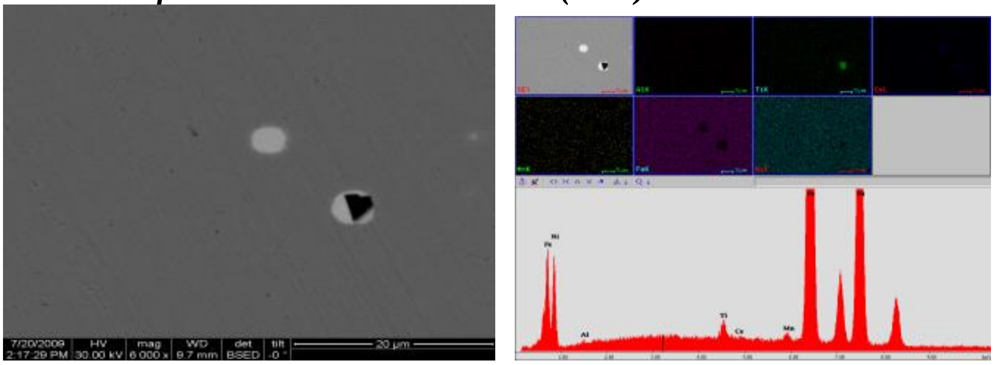

a) b)

Fig. 11. a) Titanium nitride; b) Image of backscattered electrons and distribution in surface of relative intensity of radiation X characteristic to AlKα, TiKα, MnKα , FeKα and NiKα on the micro-area from Fig. 11

Results are presented in Table 6.

*Table 6*

**Gas and sulphur concentration analysis for samples SA1 – SA5**

| Sample labelling | $O_2$ | $N_2$ | S |
|---|---|---|---|
| **SA 1** | 0.0087 | 0.0043 | 0.0104 |
| **SA 2** | 0.0080 | 0.0020 | 0.0062 |

| | | | |
|---|---|---|---|
| **SA 3** | 0.0105 | 0.0045 | 0.0115 |
| **SA 4** | 0.0092 | 0.0056 | 0.0079 |
| **SA 5** | 0.0085 | 0.0053 | 0.0103 |

## 4. Conclusions

The microscopic analysis of samples labelled SA1, SA2, SA3, SA4 allows the following conclusions: ● The kettle treatment conducted with calcium determines a decrease in inclusions concentration and dimensions reduction associated to the spheroidizing effect. ● The vacuum melting generated an important decrease of inclusions regarding their density and dimensions. It has been observed a lower distribution difference as against maraging steel treated with calcium.

From gas analysis it can be concluded that: ● Applying a vacuum treatment in case of samples tampered with Al (see SA3 and SA1) generates a drop out of 20 ppm of material. In case of the treatment with structural purification elements (Ti and Mg) the vacuum eliminates only 12 ppm from the liquid. ● In case of both kettle treatment using purification elements (Mischmetal) and vacuum method, the values for gas content are the same (0.0092 % - 0.0080 %). Likewise, there have been obtained remarkable results regarding the reduction and adapted morphology of inclusions ($Al_2O_3$, TiN). ● Mischmetal cerium manages to react with oxides and nitrites, reducing their size and creating a space around them.

## R E F E R E N C E S

[1]. *A. Rotariu, F. Bucur, G. Toader, M. Lupoae, A. Sava, P. Şomoiag, M. Cîrmaci*, Experimental Study on Polyurea Coating Effects on Deformation of Metallic Plates Subjected to Air Blast Loads, Materiale Plastice, **Vol. 53,** no. 4, 2016, pp 670-674.

[2]. *G. Roberts, G. Krauss, R. Kemedy*, Tool Stell, ASM International, USA 1998, p.1-97.

[3]. *H.F. Abreu, S.M. Tavares,* The influence of an intermediate austenitisation heat treatment in the texture of cold-rolled and aged 18 % Ni maraging steel, Mater. Charact. **Vol. 52**, 2004, p. 203–207.

[4]. *S. Fboreen*, Metall Revue, 1968, **vol.126**, p. 115-128.

[5]. *H.T. Becker, D. Dimitrov*, The achievable mechanical properties of SLM produced Maraging Steel 300 components, Rapid Prototyping J. **Vol. 22**, 2016, p. 487–494.

[6]. *A. Ardell*, Precipitation Hardening. Metall. Trans. **A (16)**, 1985, p. 2131-2165.

[7]. *Y. Asayama*, Delayed failure and precipitation behavior in maraging steels, Trans. Jpn. Inst. Met., **28 (4)**, 1987, p. 281 – 290.

[8]. *V. Berezovskaya, S.V. Grachev*, The role of texture in the processes of aging and delayed fracture of maraging steel, Metal Science and Heat Treatment, **Vol. 43**, No. 1 – 2, 2001.

[9]. *S.D. Erlach, H. Leitner*, Comparison of NiAl precipitation in a medium carbon secondary hardening steel and C-free PH13-8 maraging steel, Materials Science and Engineering, **Vol. 429**, 2006, p. 96–106.

[10]. *C. Tan, K. Zhou, M. Kuang, W. Ma, T. Kuang,* Microstructural characterization and properties of selective laser melted maraging steel with different build directions, Science and Technology of Advanced Materials. **Vol. 19**, Issue 1, 2018, p. 746-758.

[11]. *P. Würzinger, P. Rabitsch, W. Meyer*, Production of maraging steel grades and the influence of specified and nonspecified elements for special applications, Journal of Materials Science. **Vol. 39**, Issue 24, 2004, p. 7295–7302.

[12]. *C. Turk, H. Zunko, C. Aumayr, H. Leitner, M. Kapp,* Advances in Maraging Steels for Additive Manufacturing, BHM Berg- und Hüttenmännische Monatshefte, **Vol. 164**, Issue 3, 2019, p. 112–116.

[13]. *G.C. Ionescu, O.N. Ionescu, N.N.Antonescu, I.Nae*, New image processing based method for automated welding technology, Journal of the Balkan Tribological Association, **Vol.16**, no.2, 2010, pag.189-196.